Journal of Ceramic Processing Research. Vol. 11, No. 3, pp. 372~376 (2010)

J O U R N A L O F
Ceramic Processing Research

Production, microstructural comparison and mechanical behavior of reinforced alumina composites containing zirconia, silicon carbide, nickel and titanium

Enrique Pastorino-Chassale[a], Enrique Rocha-Rangel[b] and Mario Romero-Romo[c,*]

[a]*Departamento de Energia, Universidad Autonoma Metropolitana, Av. San Pablo # 180. Col. Reynosa-Tamaulipas, D. F. 02200, Mexico*

[b]*Departamento de Mecatrónica, Universidad Politécnica de Victoria Luis Caballero No. 1200, Col. Del Maestro, Cd. Victoria, Tamaulipas, 87070 México*

[c]*Departamento de Materiales, Universidad Autónoma Metropolitana, Av. San Pablo # 180. Col. Reynosa-Tamaulipas, D. F. 02200 México*

Using a mix of Al_2O_3 powders to which other reinforcing materials such as: ZrO_2, SiC, Ni and Ti were added up to 10 wt%, and the combination of conventional techniques known as milling-pressing-sintering, several composite samples were fabricated. The microstructures of the composites reinforced with (Ni or Ti) examined in the scanning electron microscope showed a slight metallic network formed between the alumina grains. The action of several mechanisms such as crack bridging, crack deflection and microcracking seems to be the cause of the improvement in the fracture toughness of the composites with respect to that of monolithic alumina. The experimental values of elastic modulus and hardness of the composites diminished, although, on the other hand, the compressive and flexural fracture strengths were increased when alumina was reinforced with the materials studied here.

Keywords: Alumina composites, Fracture toughness, Reinforcements, Metal networks.

Introduction

The increasing demand for more resistant and affordable structural components has-intensified the development of new materials and their processing technologies, although amidst these, powder mixing has clearly become a growing alternative for the elaboration of new materials. Al_2O_3 possesses favorable physical and chemical properties such as high strength, hardness and high elastic modulus. However, its application is somewhat limited due to its poor toughness in regard to that of metals, because of inherent ionic and covalent ceramic bonds. According to the results of Sekino *et al*., (1991) cited by Jiao *et al*., [1] the incorporation of small amounts of SiC particles (5-10 vol.%, 0.3 μm diameter) into an alumina matrix significantly enhanced its mechanical properties such as toughness. Since there is a great interest in the so called ceramic-ceramic and ceramic-metal (cermet) several composites have been developed. Using conventional techniques, densification is improved when the milling was increased from 1 h to 12 h in Al_2O_3/Al samples [2]. Another study of alumina/copper composite materials (with different copper contents up to 5 vol.%) fabricated by PECS (Pulse Electric Current Sintering) established that the toughness and strength enhancement up to 30% was proportionally related to the amount of copper [3]. Al_2O_3/Cu (from 5% to 30% wt) composites were fabricated by means of a conventional technique [4]; here increments in the densification due to solid and liquid copper diffusion were reported. Also, the authors reported an incipient network formation of copper particles surrounding the alumina grains, whose growth is restricted at greater weights of the reinforcement material (copper), giving higher density and higher fracture toughness. Another research study that compared two types of Ni vol.% /Al_2O_3 samples fabricated using conventional and chemical techniques [5], respectively, indicated that an almost uniform particle distribution was obtained, where the reduced particle size (~50-100 nm) impeded the achievement of significant toughness increments. Different cases of the force required to impel the crack front bowing between pores (regardless of its sizes) were studied [6]. Sometimes this effect improves the toughness of alumina composites. Also crack/particle interactions in alumina/silicon carbide nanocomposites have been investigated [1] by scanning electron microscopy and transmission electron microscopy. The researchers found predominantly transgranular fracture in the nanocomposites. The small size of the particles (~200 nm) limited increasing the toughness of the composite as compared with that of monolithic alumina. One of three types of fabrication process of composite materials (20 vol. % Ni/Al_2O_3) was designed [7] in order to produce an interconnected network of nickel particles surrounding alumina grains, which permitted one to obtain a toughness increment of 3.5 times greater than that of monolithic alumina. It was demonstrated that a significant

*Corresponding author:
Tel : +52-55-5318-9471
Fax: +52-55-5318-9087
E-mail: mmrr@correo.azc.uam.mx

effect due to partial debonding at the matrix/particle interfaces was beneficial to the composite´s toughness.

Experimental procedure

The starting materials were Al_2O_3 powder (99.5%, 1 μm, Meyer, USA), ZrO_2 powder (99%, 1 μm, Tosho, Japan), SiC powder (99%, 3 μm, Meyer, USA), Ni powder (99.5%, 3 μm, Aldrich, USA) and Ti powder (99.5%, 3 μm, Aldrich, USA). The final contents of ZrO_2, SiC, Ni and Ti in the alumina matrix were 10 weight%, respectively, to produce five samples for each composite. The final reported results express average values obtained from the evaluations with their corresponding standard deviations. The powder mixtures were ball-milled with ZrO_2 as the milling media at a 400 $minute^{-1}$ rotation speed for 12 h, with a ball-to-powder weight ratio of 20 : 1. The powder milling and mixing were controlled using isopropyl alcohol (3 ml). Subsequent to milling the powder mixes, three types of samples were fabricated by uniaxial pressing applied at 200 MPa: a) cylindrical samples 20 mm diameter × 2 mm height (for the hardness and fracture toughness tests), b) cylindrical samples 10 mm diameter × 20 mm height (for compression tests) and c) rectangular bar ($4 \times 3 \times 20$ mm^3) specimens (for elastic modulus and flexural strength tests). The pressed samples were immediately sintered at 1400 ºC for 1 h using an electrical resistance furnace provided with an inlet for supplying a nitrogen atmosphere. The nitrogen flow and the heating rate were 0.3 $m^3 minute^{-1}$ and 5 ºC $minute^{-1}$, respectively. When the sintering cycle was completed, the samples were cooled in the switched off furnace. The density of as-sintered specimens was determined through the Archimedes' method. The microstructure was investigated by scanning electron microscopy (SEM, Philips 6300). The sample hardness was evaluated using a Vickers indentation tester (1 kg for 15 s). The toughness and the length of the cracks out of the indenter´s print were estimated by the fracture indentation method [8]. The elastic modulus was determined by an ultrasonic method using a Grindo Sonic MK5 instrument. Flexural and compression strengths were measured in an Instron universal testing machine; both tests were evaluated at 0.05 mm $minute^{-1}$ machine head speed.

Results and Discussion

Densification

Table 1. shows the values of the relative density for each composite with respect to the alumina sample: comparatively, all composites attained greater density values as referred to the pure alumina. Thus, in terms of densification increases, the composites that displayed the greatest and the lowest values of this property were obtained for the titanium and the nickel composites, respectively. The apparently long milling time (12 h) diminished the particle size, which implies that the voids in the samples diminished; consequently, the mass transfer process during sintering had been improved. The melting point of the second phase is generally greater than the sintering temperature in all cases here studied, although, the melting point of nickel is closer (1455 ºC); therefore the densification increased, but the liquid phase densification enhancement associated with the second component in the composites was not generally expected.

Microstructure

The resulting microstructure of the Al_2O_3/ZrO_2 system is presented in Fig. 1(a), which displays the alumina gray phase and the ZrO_2 (generally intergranular) lighter phase. Porosity appears as a black color but its area is small enough, corresponding to the relatively high density value obtained (98.4%) in this sample. It was reported [9*] that amounts of 2.5 wt.% or more ZrO_2 in Al_2O_3/ZrO_2 composites control the alumina grain growth because of the tetragonal-monoclinic (t-m) transformation. The Al_2O_3 and ZrO_2 particle sizes in this sample after sintering were very small, about 0.6 and 0.7 μm, respectively (Table 2).

The microstructure of the Al_2O_3/SiC system is presented in Fig. 1(b); here some SiC particles (the lighter phase) surround the alumina grains, but Fig. 1(b) also shows too many SiC particles inside the alumina grains. Here the thermal expansion coefficient (TEC) of the intragranular SiC particles mismatches that of the Al_2O_3 causing the appearance of tensile residual hoop stresses during sample cooling. For such a reason, a gradual sample cooling was used (in order to avoid excessive cracking) from the sintering temperature of 1400 ºC. The ultimate strength was improved because the intragranular tensile stresses were shifted to the grain boundaries and transformed into compressive stresses. The SiC particles restricted the displacement of boundaries and thus the alumina grains diminished. On the other hand, the tensile stresses caused transgranular cracks [1] that weakened the alumina matrix and contributed to a diminishing alumina grain size also. So the configuration of the microstructure seems to be effective to improve

Table 1. Relative density and mechanical properties measured in the composites studied

System	ρ_r (%)	H_V (GPa)	K_{IC} ($MPam^{1/2}$)	E' (Theoretical) (GPa)	E (Experim.) (GPa)	Flexural strength (MPa)	Compression strength (GPa)
Al_2O_3	94.9	10.97+/–0.17	3.2+/–0.1	380	340+/–15	280+/–26	3.55+/–0.15
Al_2O_3-ZrO_2	98.4	9.87+/–0.09	4.2+/–0.1	368	330+/–13	384+/–19	4.86+/–0.14
Al_2O_3-SiC	97.3	10.64+/–0.10	4.0+/–0.1	353	352+/–12	364+/–21	4.61+/–0.16
Al_2O_3-Ni	96.4	10.21+/–0.09	3.6+/–0.1	371	335+/–13	336+/–22	4.25+/–0.13
Al_2O_3-Ti	99.2	9.17+/–0.12	3.8+/–0.1	357	348+/–12	345+/–20	4.37+/–0.17

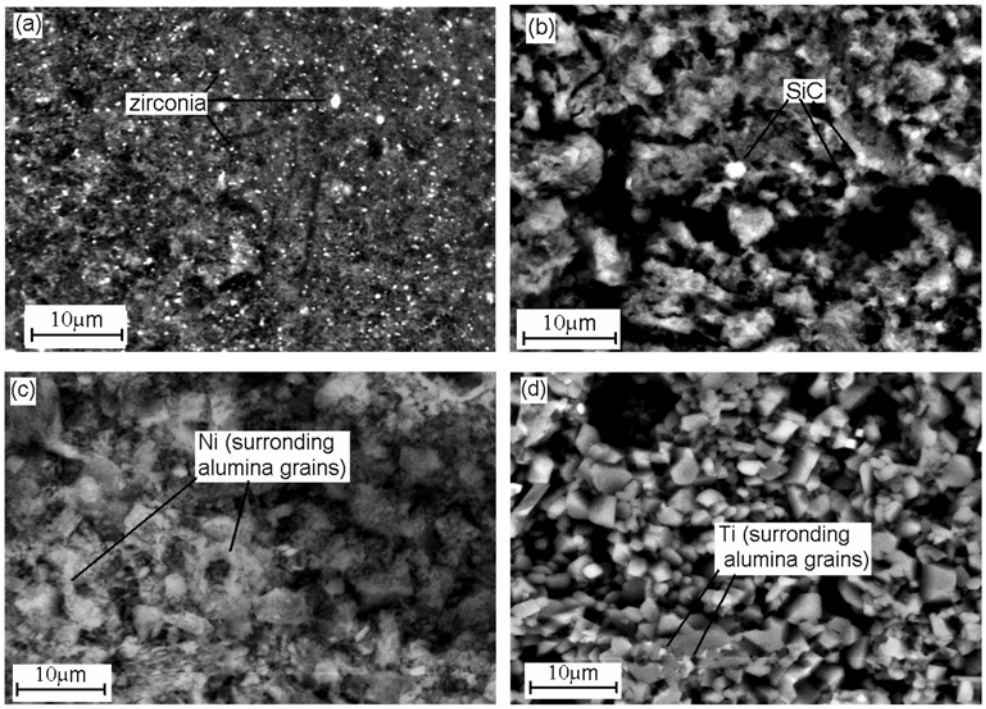

Fig. 1. SEM microstructures of sintered (1400 °C, 1 h) composites. a) Al_2O_3/ZrO_2, b) Al_2O_3/SiC, c) Al_2O_3/Ni, d) Al_2O_3/Ti.

Table 2. Grain (G) and particle (D) sizes. Measurements of G for alumina and of G and D for the composite were taken using two types of micrographs respectively, via the linear intercept method. "A" is a composite mechanical property (hardness, compression strength or flexural strength) which was calculated based on the alumina measured values

Composite	Average grain size (G, μm)	Standard deviation (%)	Average particle size (D, μm)	According to Hall-Petch relation ($A \alpha G^{-1/2}$)		
				Hardness (GPa)	Flexural strength (MPa)	Compression strength (GPa)
Al_2O_3 -ZrO_2	3.59	10.3	0.7	18.30	467	5.92
	2.55	13.3	0.6	21.72	554	7.03
Al_2O_3 -SiC	8.6	18.2	1.65	11.82	302	3.82
	6.88	13.3	1.97	13.22	337	4.27
Al_2O_3 -Ni	10.4	13.8	1.2	10.75	274	3.48
	6.53	16.8	-	13.57	346	4.39
Al_2O_3 -Ti	10	16.9	2.6	10.97	280	3.55
	6	23	1.8	14.16	361	4.58
Al_2O_3	10	-	-	10.97	280	3.55

mechanical properties. Nevertheless, in the model proposed by Sekino *et al*., [cited in 1] the large tensile stresses at the tip of the crack (near the intragranular particle) are not considered and their effect is unknown. Concerning the densification, Fig. 1(b) shows large black areas due to porosity, which is compatible with the moderate density value (97.3%) of the sample.

The microstructure of the Al_2O_3/Ni and Al_2O_3/Ti composites are presented in Figs. 1(c) and (d), respectively, where a tenuous Ni or Ti metallic network (light phases) that appears surrounding the alumina grains inhibited the grain growth according to the starting sizes of the particles. When the advancing crack meets the metallic second phase, plastic deformation is then activated, consequently there occurs deformation energy absorption by the metal, which helps to arrest further crack advancement. Furthermore, crack bridging closes the crack wake and reduces the stresses near the crack tip. Since the networks formed by metal particles are proportional to the density and weight or volume percentage of the metallic phase, it is expected that the metal thus distributed over the boundaries network should give rise to toughness improvements [7]. Then 10 wt.% Ni or Ti used in these composites is a relatively low percent, therefore, the present work nearly provided the conditions for network formation.

The bond matrix/particle in the Al_2O_3/Ni composite is strong because of the hoop compression stresses that are promoted by differences between the thermal expansion coefficients, such that TEC/Ni >> TEC/Al_2O_3 and the crack avoids the particle. In the case of Al_2O_3/Ti, neither the

difference between materials TECs nor between their elastic moduli (that is elasticity) are important, although perhaps some local microplasticity exists.

Mechanical properties

Table 1 also presents the average results and standard deviation values of the mechanical properties of the composites.

Fracture toughness

Values of the fracture toughness measured in the composites fabricated here are presented in Table 1, where it is possible to distinguish that in all the reinforced composites there is a significant enhancement of this property, as compared with monolithic alumina. For the Al_2O_3/ZrO_2 composite (Fig. 2(a)), the micrograph shows sinuous crack paths. It would appear that here the (t-m) transformation is the main toughening mechanism. Al_2O_3/SiC samples show transgranular crack paths and where the particle size (~2 μm, Table 2) is small enough in order to start microcracks: the energy dissipated increased the toughness. Crack deflection and crack bridging are the possible toughening mechanism in Al_2O_3/Ni (Fig. 2(b)) and Al_2O_3/Ti composites. For the four composites some synergy between the toughening mechanisms is not excluded. From the results analyzed, it can be possible to state that neither pore (or particle) bowing [6] nor pull out appeared as part of these experiments, because the wt.% addition and slip, respectively, are below the required threshold. Fracture toughness results were better in the ceramic-ceramic composites than in the cermets, as exemplified by the Al_2O_3/ZrO_2 composite where the t-m transformation was the main mechanism controlling the toughness improvement. After this, it can be argued that in order to improve the toughness of cermets, a suitable metallic network build up is recommended as part of the fabrication process design. Another way is increasing the dispersion vol. or wt.%.

Elastic modulus

Theoretical (rule of mixtures) and experimental values of the elastic moduli (E' and E respectively) were determined (always E' > E, Table 1). From this table it seems clear that densification is proportional to the elastic modulus except for the Al_2O_3/ZrO_2 composite; the experimental value of E is almost the same with respect to the Lange's graph according to reference [10]. The experimental E diminished due to microcracks mainly caused by the transformation of the zirconia. With respect to the remaining composites, the porosity seems to be the principal factor for diminishing the elastic modulus. However the E-porosity correlation was not verifiable due to the high densification obtained for the composites in this study.

Hardness

It is a well known fact that in polycrystalline materials slip is much more important than twinning. Thus H ~0.08 G (H and G~150 GPa are hardness and shear modulus for monolithic alumina respectively). Consequently H = 12 GPa, is a near enough value, that is shown in Table 1. Thus twinning seems not to be significant. In the case of the Al_2O_3/Ni composite using the Cok-Pharr relation [11], H_v = 13.5 GPa versus 10.21 GPa (experimental value) according to Table 1, considering P (indentation load) = 1 kg and 2a (indentation diagonal length) = 38 μm. By the rule of mixtures and the Hall-Petch relation [9**] the calculated hardness values of the composites were 5-22% and ~30% higher, respectively, than the experimental results, except in the case of Al_2O_3/ZrO_2 (only for the Hall-Petch relation), where the theoretical value was ~ twice the experimental value due to the small grain size (Table 2). The local porosity not considered in the Hall-Petch relation perhaps justifies the difference between theoretical and experimental values.

Flexure and compression fracture strength

Composite flexure and compressive fracture strength were moderately improved, as indicated by the following results: Al_2O_3/ZrO_2 37%; Al_2O_3/SiC 30%; Al_2O_3/Ni 20% and Al_2O_3/Ti 23%. For both the flexural and compressive fracture strengths, the small grain size of the Al_2O_3/ZrO_2 theoretical values as determined by the Hall-Petch method are much larger than the experimental results, whereas, for the Al_2O_3/SiC, Al_2O_3/Ni and Al_2O_3/Ti composites, the

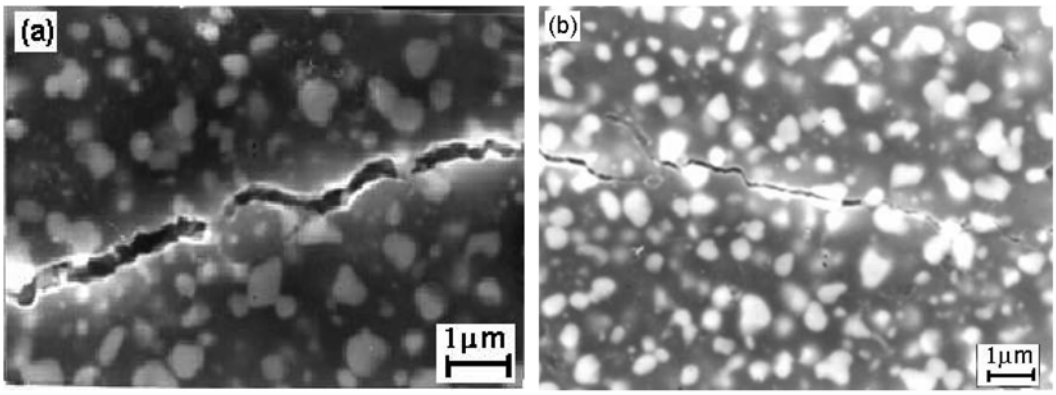

Fig. 2. Secondary electron images from the scanning electron microscope taken to reveal the crack path in (a) Al_2O_3-ZrO_2 and (b) Al_2O_3-Ni composites, respectively.

theoretical and experimental results acceptably agreed. The compression strength of alumina (Y) estimated using Y = H/3 was 3.66 GPa, with H = 10.97 GPa versus 3.55 GPa (Table 1).

Conclusions

- Densification of the four composites was increased over that of alumina.
- Cermet composite microstructures show a tenuous metallic network surrounding alumina grains. In addition, in every case (Al_2O_3 with ZrO_2, SiC, Ni or Ti) alumina grain sizes remain very fine.
- Referring to mechanical properties, the toughness of the four composites was improved significantly in regard to monolithic alumina. The ZrO_2 (t-m) transformation was the main crack arrest mechanism but microcracks were also expected. Deflection cracks and crack bridging exist except for the Al_2O_3/SiC composite. The difference in TEC's increased the toughness of some composites via hoop stresses. Neither pore or particle bowing nor pull out was expected. Experimental elastic moduli diminished, sometimes strongly, with respect to the theoretical prediction, principally by microcracks in Al_2O_3/ZrO_2 and a pore effect in Al_2O_3/SiC, Al_2O_3/Ni and Al_2O_3/Ti. The hardness of composites was lower than that of monolithic alumina. However, flexural and compressive strengths improved in every composite and comparing values between experimental and theoretical results (using the Hall-Petch relation) some differences between them were found.

Acknowledgements

ERR and MARR wish to express their thanks to the SNI for the distinction of their membership and the stipend received. MARR wishes to thank the Departamento de Materiales at UAM-A for the financial support given through project 2260235.

References

1. S. Jiao, M.L. Jenkins and R.W. Davidge, Journal of Microscopy, 185 (1997) 259-264.
2. E. Rocha-Rangel W, López-Yépez, M. Romero-Romo and E Garciafigueroa-Medina; Ceram. Eng. & Sci. Proce., 22 (2001) 84-88.
3. S.J. Ko, K.H. Ming, Y.D. Kim and I.-H. Moon, J. Am. Ceram.Soc., 3 (2002) 192-194.
4. J.G. Miranda-Hernández, S. Moreno-Guerrero, A.B. Soto-Guzmán and E. Rocha-Rangel, Journal of Ceramic Processing Research, 7 (2006) 1-5.
5. T. Sekino, T. Nakajima, S. Ueda and K. Niihara, J. Am. Ceram. Soc., 80 (1997) 1139-1148.
6. J. Wang, L.J. Vandeperre, R.J. Stearn and W.J. Clegg, Journal of Ceramic Processing Research, 2 (2001) 27-30.
7. M.M. El-Sayed Seleman, J. Mater. Sci. Technol., 24 (2008) 723-728.
8. A.G. Evans and E.A. Charles, J. Am. Ceram. Soc., 59 (1976) 371-373.
9. R.W. Rice, Mechanical Properties of Ceramics and Composites, Marcel Dekker Inc. New York, (2003) 551 *, 246**.
10. D.J. Green, R.H. J Hannink, and M.V. Swain "Transformation Toughening of Ceramics" CRC Press, Inc. Boca Ratón, Florida, (2002) 166.
11. John B. Watchman, "Mechanical properties of ceramics" John Wiley and Sons Inc, NY, (1996) 84.